

isotope effect was first advocated by Robertson and co-workers about one and one-half decades ago,¹⁵ and very recently has received support from theoretical calculations by van der Zwan and Hynes.²⁹

Experimental Section

Materials. Aldrich spectrophotometric grade CH₃CN [(H₂O) ≈ 0.01 M by Karl Fischer titration] was used without further purification in preparing solutions with high water concentrations ([L₂O] > 1 M). For use in preparing solutions with lower water concentrations, 100-mL samples of this CH₃CN were dried by two successive bulb-to-bulb distillations on a vacuum line from 12-g portions of freshly activated (>3 h at *T* > 300 °C and *P* < 10⁻³ torr) 3-Å molecular sieve. Karl Fischer titration of this dried CH₃CN indicated [H₂O] << 10⁻³ M. This low water content was confirmed by drying a sample of CH₃CN which contained 1 M D₂O (three successive distillations from portions of 3-Å sieve which had been wetted with D₂O before being activated); the agreement (see Figures 2 and 3) of K_a^H/K_a^D values measured by using this CH₃CN as solvent with those measured by using other dried samples of CH₃CN indicates [L₂O] ≤ 10⁻⁴ M in both solvents. The H₂O used was ordinary distilled water which had been passed through a Barnsted 0808 mixed-bed ion-exchange column. Aldrich D₂O (99.8 atom % D) was used without further purification. A stock solution of DClO₄ was prepared from 70% HClO₄ by repeatedly adding D₂O and distilling off the excess L₂O in vacuo; the residual H content was measured by ¹H NMR spectroscopy. A corresponding stock solution of HClO₄ was prepared by distilling the excess H₂O from 70% HClO₄ in vacuo; the compositions of the constant-boiling deuterio and protio acids which remained in the pot were both very close to LCIO₄·2L₂O; these compositions were checked by titration. Kodak *N,N*-dimethyl-*p*-nitroaniline (1) was recrystallized from ethanol. *N,N*-Dimethyl-3,5-dinitro-4-toluidine (2) was prepared as described³⁰ and recrystallized from heptane: mp 90.5–92 °C. 4-Chloro-*N,N*-dimethyl-2,6-dinitroaniline (3) was prepared by the reaction of 1,4-dichloro-2,6-dinitrobenzene³¹ with dimethylamine

(29) van der Zwan, G.; Hynes, J. T. *J. Chem Phys.* **1982**, *76*, 2993–3001; **1983**, *78*, 4174–4185.

(30) Pinnow, J.; Matcovich, A. *Chem. Ber.* **1898**, *31*, 2514–2523.

(31) Matsumoto, I. *Yakugaku Zasshi* **1965**, *85*, 544–546. (*Chem. Abstr.* **1965**, *63*, 6898.)

and was recrystallized from methanol: mp 110.5–111 °C.

p*K*_a Measurements. The dissociation constants (K_a^H and K_a^D) for the conjugate acids of indicators 1, 2, and 3 were measured by UV spectrometry. Absorbance measurements of 1, 2, and 3 were made at 395, 430, and 430 nm, respectively; the conjugate acids of 1, 2, and 3 do not absorb at these wavelengths. Absorbances were measured for sets of four cells in the thermostated (25.0 ± 0.1 °C) carousel of a Varian Cary 219 spectrophotometer. Two cells in each set contained CH₃CN, H₂O, and indicator; one of these two also contained HClO₄. The other two cells were set up analogously, D₂O and DClO₄ being substituted for H₂O and HClO₄; the total numbers of formula weights of CH₃CN, D₂O, DClO₄, and indicator in each cell in the deuterio pair were equal to those of CH₃CN, H₂O, HClO₄, and indicator in the protio pair. Within each pair, the value of the extinction coefficient of the indicator base at that L₂O concentration was calculated from the absorbance of the cell which lacked LCIO₄, and this value was used, together with the absorbance of the acidic solution and the known total amounts of indicator and LCIO₄, to evaluate the molarities of L⁺, indicator base (B), and indicator conjugate acid (BL⁺) needed for the evaluation of K_a^L via eq 3. Small amounts of H (<10 atom %) were present in the D solutions (mostly from the DClO₄ stock which was 91 atom % D). The apparent value of $(K_a^D/K_a^H)^{1/3}$ was corrected for the presence of that H by the approximate equation $(K_a^D/K_a^H)^{1/3} \approx [n - 1 + (K_a^D/K_a^H)^{1/3} \text{app}]/n$, where *n* is the atom fraction of D.

Special precautions were taken in preparing samples with total [L₂O] ≤ 0.2 M: glassware and cells were dried in a vacuum oven and allowed to cool in Ar; all transfers were by syringe through serum caps, and vapor spaces above solutions were maintained at 1 atm of Ar. Samples and intermediate dilutions were used immediately after preparation to avoid errors arising from a slow decrease in acidity (presumably caused by the hydrolysis of CH₃CN in these extremely acidic solutions).

Acknowledgment. This work was supported in part by Grant CHE83-04874 from the National Science Foundation.

Registry No. CH₃CN, 75-05-8; H₃O⁺, 13968-08-6; D₂, 7782-39-0; *N,N*-dimethyl-*p*-nitroaniline, 100-23-2; *N,N*-dimethyl-3,5-dinitro-4-toluidine, 91266-70-5; 4-chloro-*N,N*-dimethyl-2,6-dinitroaniline, 10156-68-0.

On the Magnitude of Primary Isotope Effects for Proton Abstraction from Carbon

D. J. Hupe* and E. R. Pohl

Contribution from Merck Sharp and Dohme Research Laboratories, Rahway, New Jersey 07065, and Department of Chemistry, University of Michigan, Ann Arbor, Michigan 48109.

Received January 30, 1984

Abstract: Primary deuterium isotope effects have been measured for the loss of an α proton from 4-(4-nitrophenoxy)-2-butanone. The isotope effect data showed that no significant change in transition-state structure occurred in the same region of oxyanion catalyst p*K*_a range that does exhibit a large change in β value. This confirms the previous assertion that the dramatic curvature in the Brønsted plot for proton abstraction by oxyanions from carbon is due to solvation. The effect upon k_H/k_D of varying the identity of the atom acting as the proton acceptor was examined. Catalysts having oxygen, nitrogen, carbon, and sulfur as the acceptor atom were included. An inverse correlation was found between the magnitude of the isotope effect for proton abstraction by X⁻ and the energy change upon conversion of HX to DX. With use of the Marcus equation as a basis, an equation was derived for predicting values of k_H/k_D which not only relies on the Δ*pK*_a value but also incorporates the zero-point energy difference of both the reactants and the products as measured by infrared stretching frequency shifts upon deuteration. This equation gives an improved correlation between calculated and experimental values of k_H/k_D taken from the literature.

We have previously demonstrated¹ that Brønsted plots for proton abstraction from carbon acids by oxyanions in aqueous solution exhibit pronounced curvature, such that highly basic oxyanions are nonselective (β = 0.2) whereas weakly basic oxyanions are very selective (β = 0.8). We have proposed that this

curvature is caused by an effect due to solvation rather than by a Hammond postulate type of change in transition-state structure. Consistent with this argument is the fact that when thiol anions abstract protons from carbon they do not exhibit the Brønsted plot curvature or rate enhancement due to solvation that is found

* Address correspondence to this author at Merck Sharp and Dohme.

(1) Hupe, D. J.; Wu, D. J. *Am. Chem. Soc.* **1977**, *99*, 7653.

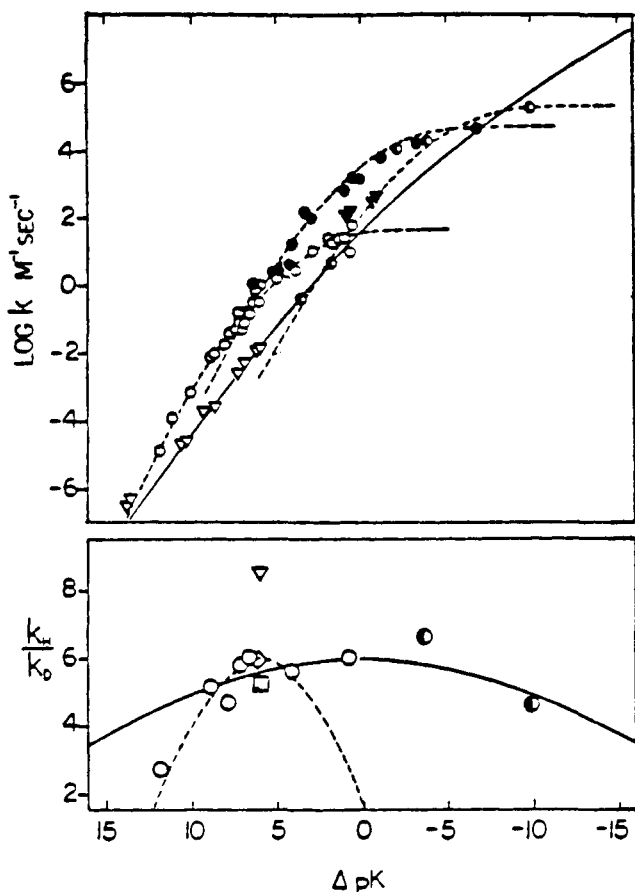


Figure 1. The upper plot shows rate data for oxyanion and thiol anion catalyzed proton abstraction from 4-(4-nitrophenoxy)-2-butanone (○, ▽), acetylacetone (●, ▼), and ethyl nitroacetate (◐). The lower plot shows values of k_H/k_D for oxyanions (○), amine (◇), and thiol anion (▽) with 4-(4-nitrophenoxy)-2-butanone and oxyanions with ethyl nitroacetate (◐). The solid line is the type of dependence expected for a large intrinsic barrier (10 kcal/mol). The dashed line is the type of dependence expected for a small intrinsic barrier (2.5 kcal/mol).

for oxyanions,² as demonstrated in Figure 1. These data were obtained in aqueous solution by using 4-(4-nitrophenoxy)-2-butanone, (**1**) as substrate because the general base catalyzed proton transfer of interest is followed by expulsion of *p*-nitrophenoxide so that the reaction is easily studied spectrophotometrically.¹ Because the proton transfer is slower than the expulsion and because the two steps are essentially uncoupled mechanistically (an irreversible carbanion mechanism), the data are comparable to enolization rates measured by other, more cumbersome methods.³

A useful index of transition-state structure is the primary deuterium isotope effect.⁴ A number of studies,⁵⁻¹² particularly those of Bell, indicated that there is a maximum for k_H/k_D when the pK_a of the proton abstractor and the carbon acid are equivalent, thus confirming the prediction of Westheimer.¹³ Though badly scattered,¹⁴ plots of k_H/k_D suggested that a change of 30–40 ΔpK_a

units would be required to change the value of β from 0.2 to 0.8. This type of gradual change in β with ΔpK_a was measured by Bell¹⁵ when a series of carbon acids was studied with a homologous series of catalysts. In terms of the Marcus formulation,¹⁶⁻¹⁸ a large intrinsic barrier of about 10 kcal is required to describe these gradual changes in β and k_H/k_D with pK_a , and the solid lines in the top and bottom of Figure 1 were computed by using this value. An apparent intrinsic barrier of only 2.5 kcal would be required to match the dramatic Brønsted plot curvature found for oxyanions with **1**,¹ as shown by the dashed lines in Figure 1. We wanted to measure values of k_H/k_D for **1** in this study so that we might confirm our interpretation of solvation as the cause for Brønsted plot curvature in the only experimental case where a complete set of rate data are available demonstrating such curvature. If solvation rather than a change in the degree of proton transfer were responsible for the variation in β then k_H/k_D values should change very little with the basicity of the oxyanion during the proton abstraction. The dashed line in the lower panel of Figure 1 shows the dependence of k_H/k_D expected if the measured β values for oxyanions with **1** reflected the degree of proton transfer.

Another point that we wished to examine was the dependence of k_H/k_D on the identity of the proton-abstracting base. It is common practice to measure series of rates or isotope effects by using a given carbon acid and a homologous series of catalysts such as amines or acetates. These series often show a logical increase in k_H/k_D as ΔpK_a approaches 0 but gives unpredictable changes when bases of different types are used. We wished to measure, therefore, the isotope effect for the reaction of **1** with acetate, substituted phenoxides, alkoxides, and hydroxide ion as well as an amine, a thiol anion, and cyanide ion.

Experimental Section

Synthesis of 1-d. Dimethyl (2,2-²H₂)Malonate (3).¹⁹ Methylene chloride (75 mL), (*O,O*,2,2-²H₄)malonic acid (17.06 g, 0.158 mol), (²H₁)methanol (25 g, 0.176 mol), and (²H₂)sulfuric acid (0.5 mL) were placed into a flask which had been rinsed with deuterium oxide (5 mL), dried in an oven (130 °C, 2 h), and cooled under nitrogen. After the mixture was left to stand for 24 h, the organic phase was separated, washed with deuterium oxide (2 × 10 mL), and evaporated under reduced pressure and the resulting oil was distilled under reduced pressure (76–78 °C (10 mmHg)) to give **3** (14.9 g, 71%); NMR (DCCl₂) δ 3.73 (s); IR ν_{\max} (neat) 2960, 1760, 1540, 1260, 1090, 1041 cm⁻¹.

1,3-(2,2-²H₂)Propanediol (4).²¹ Dimethyl (2,2-²H₂)malonate (**3**) (10.5 g, 78 mmol) in ether (175 mL) was added dropwise to a solution of purified lithium aluminum hydride (4.0 g, 0.10 mol) in ether (125 mL) at room temperature and refluxed for 6 h. After the mixture was stirred overnight, a sodium hydroxide solution (0.72 g in 15 mL of water) was slowly added over 4 h, the mixture was filtered, and the yellow solid was washed with ether (50 mL) and tetrahydrofuran (50 mL). The solid residue was then refluxed three times with tetrahydrofuran (70 mL), filtered, and washed with ether (50 mL). The organic fractions were combined and evaporated under reduced pressure to give a yellow oil, which was distilled under reduced pressure (48–52 °C (12 mmHg)) to give **4** (2.56 g, 42%); NMR (acetone-*d*₆) δ 2.97–3.37 (m, 4 H), 3.63–3.97 (m, 2 H); IR ν_{\max} (neat) 3340, 2930, 2882, 2203, 2122, 1475, 1430, 1380, 1323, 1268, 1168, 1108, 1045, 1010 cm⁻¹.

3-(4-Nitrophenoxy)-1-(2,2-²H₂)propanol (5). Sodium metal (0.15 g, 6.5 mmol) was allowed to react with **4** (2.3 g, 30 mmol), and then 4-nitrofluorobenzene (1.0 g, 7.1 mmol) was added and the mixture heated for 3 h at 105 °C.²¹ After the mixture was left to stand overnight, the reaction mixture was extracted with ether (3 × 10 mL) and the ether fractions were combined, washed with cold water (6 mL), dried over anhydrous sodium sulfate, filtered and evaporated. The pale green oil was further purified by chromatography over silica gel (30 g) eluting with ethyl acetate to yield pure **5** as an oil (695 mg, 54%). The analysis was satisfactory. NMR (acetone-*d*₆) δ 3.53–3.97 (m, 3 H), 4.17 (s, 2 H), 6.93 (d, 2 H), 8.03 (d, 2 H); IR ν_{\max} (neat) 3380, 3118, 3080, 2935, 2890,

(14) Reference 4, p 224.

(15) Bell, R. P. "The Proton in Chemistry"; Cornell University Press: Ithaca, New York, 1973; p 203.

(16) Marcus, R. A. *J. Phys. Chem.* **1968**, 891.

(17) Cohen, A. O.; Marcus, R. A. *J. Phys. Chem.* **1968**, 4249.

(18) Koepl, G. W.; Kresge, A. J. *J. Chem. Soc., Chem. Commun.* **1973**, 371.

(19) Lembert, J. *J. Am. Chem. Soc.* **1967**, 89, 1840.

(20) Burns, R. C.; England, B. *J. Chem. Soc. B* **1966**, 864.

(21) Eisenbraun, E. *J. Org. Synth.* **1965**, 45, 28.

(2) Pohl, E.; Hupe, D. J. *J. Am. Chem. Soc.* **1978**, 100, 8130.

(3) Banford, C. H.; Tipper, C. F. H., Eds. "Comprehensive Chemical Kinetics"; Elsevier: Amsterdam, 1977; Vol. 8, Chapter 2.

(4) Caldin, E. F.; Gold, V., Eds. "Proton Transfer Reactions"; Chapman and Hall, Ltd.: London, 1975; Chapters 7 and 8.

(5) Bell, R. P.; Crooks, J. C. *Proc. R. Soc. London, Ser. A* **1965**, 286, 285.

(6) Bell, R. P.; Goodall, D. M. *Proc. R. Soc. London, Ser. A* **1966**, 294, 273.

(7) Barnes, D. J.; Bell, R. P. *Proc. R. Soc. London, Ser. A* **1970**, 318, 421.

(8) Riley, T.; Long, F. A. *J. Am. Chem. Soc.* **1962**, 84, 522.

(9) Dixon, J.; Bruce, T. C. *J. Am. Chem. Soc.* **1970**, 92, 905.

(10) Davis, M. H. *J. Chem. Soc., Perkin Trans. 2* **1974**, 1018.

(11) Keefe, J. R.; Munderlock, N. *J. Chem. Soc., Chem. Commun.* **1974**, 17.

(12) Rietz, O.; Kopp, J. Z. *Phys. Chem., Abt A*, **1939**, 184, 429.

(13) (a) Westheimer, F. H. *Chem. Rev.* **1961**, 61, 265. (b) Melander, L. "Isotope Effects on Reaction Rates"; The Ronald Press: New York.

Table I. Primary Deuterium Isotope Effects for the Proton Abstraction from 4-(4-Nitrophenoxy)-2-[3,3- L_2]butanone by Oxyanions, Thiol Anions, Amine, and Cyanide in Aqueous Solution at 25 °C, $\mu = 1.0$

base	pK_a	pH	concn range, M	k , $M^{-1} s^{-1}$, for 1d	k_H/k_D
HO^-	15.75		$(0.565-7.98) \times 10^{-4}$	7.97	6.13
$CF_3CH_2O^-$	12.37 ^a	10.902	$(0.675-10.9) \times 10^{-3}$	3.23	5.00
		10.985	$(0.993-13.9) \times 10^{-3}$	2.45	5.57
4- $CH_3OC_6H_4O^-$	10.06 ^a	9.532	$(0.623-6.23) \times 10^{-2}$	0.121	5.85
$C_6H_5O^-$	9.86 ^a	9.830	$(0.861-3.02) \times 10^{-2}$	8.78×10^{-2}	6.09
4- $CH_3CONHC_6H_4O^-$	9.49 ^a	9.752	$(2.83-4.82) \times 10^{-2}$	6.81×10^{-2}	5.77
3,4- $Cl_2C_6H_3O^-$	8.51 ^a	9.443	$(0.622-6.44) \times 10^{-2}$	2.50×10^{-2}	4.72
3,4,5- $Cl_3C_6H_2O^-$	7.68 ^a	8.852	$(0.186-1.95) \times 10^{-2}$	9.55×10^{-3}	5.07
CH_3COO^-	4.76 ^a	6.519	$(0.240-2.46) \times 10^{-1}$	7.19×10^{-6}	2.68
$HOCH_2CH_2S^-$	9.61 ^b	9.327	$(0.333-3.55) \times 10^{-1}$	3.75×10^{-3}	8.51
$(CH_3)_3N$	9.76 ^c	9.242	$(0.112-1.15) \times 10^{-3}$	1.60×10^{-1}	5.17
CN^-	9.21 ^b	9.497	$(0.852-8.51) \times 10^{-1}$	4.62×10^{-4}	5.86

^a Reference 1. ^b Reference 30. ^c Reference 31.

2220, 2130, 1595, 1500, 1340, 1300, 1262, 1175, 1113, 1036 cm^{-1} .

3-(4-Nitrophenoxy)(2,2- 2H_2)propanoic Acid (6). Chromium trioxide solution (0.436 g, 4.3 mmol in 0.80 mL of deuterium oxide and 0.37 mL of (2H_2)sulfuric acid) was added to (2H_6)acetone (20 mL), and a solution of **5** (0.451 g, 2.26 mmol) in 10 mL of (2H_6)acetone was added dropwise over a 3-h period and stirred an additional 3 h.²² A few drops of 2-propanol was added to destroy excess oxidant, the mixture was filtered, and the bluish-green solid was washed with methylene chloride (2×10 mL). The organic fractions were combined, dissolved in methylene chloride (100 mL), and washed with water (2×15 mL). The aqueous layer was washed with methylene chloride (25 mL), and the organic fractions were combined, dried (anhydrous sodium sulfate), and evaporated under reduced pressure to yield pure **6** (0.400 g, 96%): mp 116–118 °C, analysis satisfactory. NMR (acetone- d_6) δ 4.43 (s, 2 H), 7.10 (d, 2 H), 8.13 (d, 2 H); IR ν_{max} (KBr) 3070, 2920, 2680, 2580, 2118, 1680, 1588, 1520, 1491, 1452, 1408, 1385, 1340, 1308, 1250, 1160, 1108, 1048 cm^{-1} .

4-(4-Nitrophenoxy)-2-(3,3- 2H_2)butanone (1d).²³ Oxalyl chloride (0.21 mL, 2.5 mmol) was added to a solution of **6** (250 mg, 1.2 mmol in 15 mL dry benzene), and the mixture was refluxed for 1.5 h, cooled, evaporated under reduced pressure, twice dissolved in ether (2 mL), and evaporated under reduced pressure to yield acid chloride **7** as an oil. Without further purification, **7** was added to a solution of a 2.5 molar excess of distilled diazomethane in ether solution. After the mixture was left to stand at room temperature for 1 h, the excess diazomethane and solvent were removed by passing a stream of nitrogen over the solution and then through an acetic acid-ether trap which left behind crude 1-diazo-4-(4-nitrophenoxy)-2-(3,3- 2H_2)butanone (**8**). After recrystallization from ether, **8** (180 mg, 0.75 mmol, mp 92.8–94.2 °C) was dissolved in acetone (1 mL). An excess (2 mL) of 38% hydroiodic acid²⁴ was slowly added, and the mixture was stirred for 3 min. The reaction mixture was then dissolved in ether (30 mL), washed with 10% sodium bisulfite (10 mL), dried (anhydrous sodium sulfate), and evaporated to yield crude **20**. A pure sample was obtained by recrystallization from ether (42 mg, 16% from **6**): mp 67.5–68.8 °C; analysis satisfactory. NMR ($DCCl_3$) δ 2.27 (s, 3 H), 4.33 (s, 2 H), 6.93 (d, 2 H), 8.08 (d, 2 H); IR ν_{max} (KBr) 3100, 2940, 1711, 1592, 1511, 1495, 1455, 1340, 1300, 1262, 1180, 1103, 1021 cm^{-1} .

Kinetics. The rates of reaction of the various catalysts were measured by using previously described procedures^{1,2} at 25 °C, $\mu = 1.0$ in aqueous solution. The values of k_{obsd} measured at each concentration were plotted vs. the free base concentration of the catalyst which was computed from the pH and the pK_a . In Figure 2 a typical example is shown with use of 3,4-dichlorophenoxide as the catalyst. In some instances the absolute rate constant varied a small amount from the previously reported value, but the measurements of k_{obsd} for **1** and **1d** in this study were performed at the same time and under identical experimental conditions. In those few cases, such as acetate and cyanide, for which it was necessary to use initial rates, **1d** was first allowed to react with hydroxide ion to the extent of 1 half-life in order to ensure that little contaminating **1** remained. The resulting solution was acidified and extracted with ether several times, and then nitrogen was passed through to remove the remaining ether.

An attempt was made to measure a k_H/k_D value for cyanide that was not entirely successful. It was necessary to measure the equilibrium constant for cyanhydrin formation with **1** or **1d** so that the apparent rate constant (which in fact is negative) may be corrected, as previously

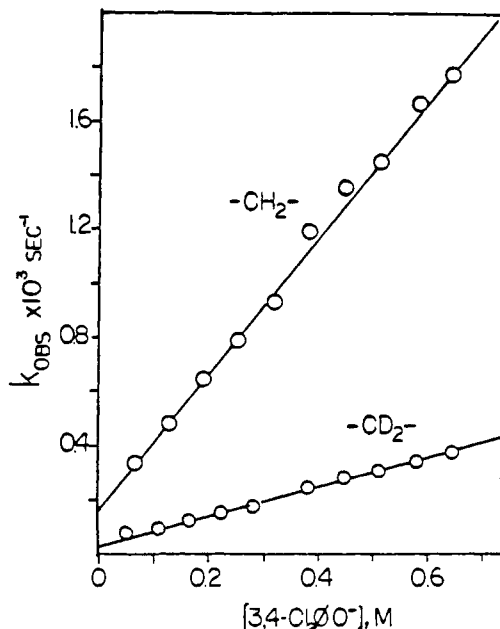
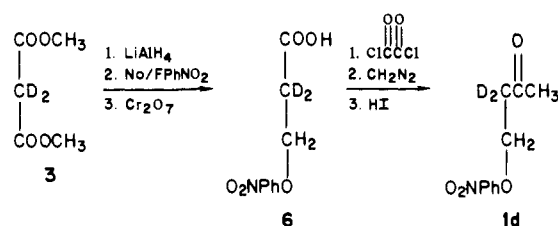


Figure 2. A plot of k_{obsd} vs. concentration of 3,4-dichlorophenol for 4-(4-nitrophenoxy)-2-(3,3- L_2)butanone showing a value of $k_H/k_D = 4.72$. Comparable experiments were performed for the other catalysts listed in Table I.

Scheme 1



described.² Because of the propensity of solutions of cyanide ion to polymerize and turn yellow, substantial error was introduced. The value of the cyanhydrin formation constant was substantially different than that measured previously ($17 M^{-1}$ compared to $26 M^{-1}$), and the value of k_H/k_D obtained is, therefore, only approximate.

Results

The nondeuterated substrate, 4-(4-nitrophenoxy)-2-butanone (**1**) was prepared as previously described.² The α -deuterated substrate, **1d**, was synthesized from dimethyl dideuteriomalonate (**3**), as shown in Scheme 1.

The values obtained from the ratios of slopes of plots of k_{obsd} values vs. concentrations of the base are listed in Table I. The value for cyanide is an approximation.

Discussion

In the Marcus formalism,¹⁻⁴ shown in eq 1, the free energy of activation ΔG^\ddagger is the sum of the work term, W_r , reflecting the

(22) Motiu-DeGroot, R.; Hunt, W.; Wilde, J.; Hupe, D. J. *J. Am. Chem. Soc.* **1979**, *101*, 2182.

(23) Shimomura, H.; Katsube, J.; Matsui, M. *Agric. Biol. Chem.* **1975**, *39*, 657.

(24) Hall, H. K. *J. Am. Chem. Soc.* **1957**, *79*, 5441.

energy required to bring the reactants together, and a function dependent upon the free energy for the proton transfer portion of the reaction, $\Delta G^{\circ'}$. If it is assumed that $W_r = W_p$ (where

$$\Delta G^{\circ} = \frac{\lambda}{4} \left(1 + \frac{\Delta G^{\circ'}}{\lambda_H} \right)^2 + W_r \quad (1)$$

$$\Delta G^{\circ} = \Delta G^{\circ'} - W_r + W_p$$

W_p is the work term for the products in the reverse reaction) then the experimentally measurable equilibrium constant, ΔG° , equal to $-RT \ln \Delta pK_R$, may replace $\Delta G^{\circ'}$ in eq 1. This equation therefore allows a fit of data in a curved plot of $\log k$ vs. $\log K_{eq}$ to be carried out in a way that divides the free energy of activation into the part that is dependent upon the equilibrium constant and the part that is not. Within this context, Brønsted plots for proton transfer which show a substantial degree of curvature over $\sim 10 \Delta pK$ units translate into small values of $\lambda/4$ (~ 2 kcal) and large values of W_r (~ 10 kcal). If the Brønsted plot has little or no curvature over the range of $10 \Delta pK_a$ units these values become large for $\lambda_H/4$ (~ 10 kcal) and small for W_r (~ 2 kcal). We have been interested in demonstrating that solvation effects can alter β values dramatically within the experimentally accessible range of $10\text{--}12 \Delta pK_a$ units typical for a series of oxyanion or amine catalysts with a single carbon acid. Data of this type give apparent small values of $\lambda_H/4$ and apparent large values of W_r , and the value of β is not 0.5 where $\Delta G^{\circ} = 0$, as is normally expected. If instead, however, a series of carbon acids is used with a homologous set of catalysts such as pyridines, then a gradual change in slope is found consistent with a large value of $\lambda/4$ (on the order 10 kcal) and a small value of W_r (on the order of 2.5 kcal) with $\beta = 0.5$ when $\Delta G^{\circ} = 0$. Interestingly, thiol anions do not exhibit the curvature due to solvation that oxyanions display with a single carbon acid.²

Equation 2 was obtained by modification of eq 1 and contains the inherent "Westheimer postulate" notion¹³ that the value of k_H/k_D will be maximized when the transition state is symmetrical, that is when $\Delta G^{\circ} = 0$ and $\beta = 0.5$. The value of $(k_H/k_D)_{max}$ is

$$\frac{k_H}{k_D} = \exp \left\{ \left(\frac{\lambda_D - \lambda_H}{4RT} \right) \left(1 - \frac{(\Delta G^{\circ})^2}{\lambda_H \lambda_D} \right) \right\} \quad (2)$$

$$(\lambda_D - \lambda_H) = 4RT \ln (k_H/k_D)_{max}$$

an adjustable parameter. The isotope effect for hydroxide, alkoxide, and phenoxide ion catalyzed proton abstraction from carbon measured in this study supports the notion that there is little change in the degree of proton transfer with the ΔpK_a range attainable by changing oxyanion catalysts.^{1,2} Thus, even though there is a very large change in the measured β value for each series of oxyanions with a single carbon acid as shown in Figure 1, the expected change in k_H/k_D , having a maximum where $\beta = 0.5$, predicted by eq 2 is not found. The dashed line in the plot of k_H/k_D in Figure 1 shows the calculated values of k_H/k_D with use of eq 2 and the measured β values for **1** with oxyanions. It is apparent that the β value reflects more than just the degree of bond formation in the transition state. The k_H/k_D data fit well (along with the hydroxide and phenoxide points for ethyl nitroacetate)⁷ on a curve with a large intrinsic barrier of approximately 10 kcal, as shown in Figure 1. This kind of gradual change in k_H/k_D with a maximum at $\Delta pK_a = 0$ has been demonstrated previously for a collection of a large number of k_H/k_D points vs. ΔpK_a , albeit with a large amount of scatter due to the variety of types of bases and carbon acids used.¹⁵ These isotope effect data provide further experimental support for the proposal^{1,2} that β values for proton abstraction by oxyanions are perturbed severely by solvation in a way that thiol anions are not perturbed.

Shown in Table III are a series of literature measurements of k_H/k_D along with the data obtained in this study. These data were fit to eq 2 with two adjustable parameters, the intrinsic barrier, $\lambda_H/4$, and the maximum value of the isotope effect, $(k_H/k_D)_{max}$. With use of a SAS nonlinear least-squares fit, the best values were $\lambda_H/4 = 5.85$ kcal/mol and $(k_H/k_D)_{max} = 8.58$. The fit of ex-

Table II. Infrared Spectral Data for Some Model Compounds

compound ^a	$\nu_{X-H} - \nu_{X-D}$	$\Delta(\nu_{X-H} - \nu_{X-D})$	$\Delta\epsilon$, kcal/mol
HF ^b	3962–2607	1355	3.87
CH ₃ CO ₂ H ^c	3583–2642	941	2.69
CH ₃ OH ^d	3682–2485	962	2.75
C ₆ H ₅ OH ^e	3653–2695	958	2.73
NH ₄ BF ₄ ^{f,h}	3332–2486 ^g	846	2.42
C ₆ H ₅ NHBF ₄ ^{f,h}	3250–2450	800	2.29
CH ₃ COCH ₃ ⁱ	3004–2255	749	2.14
CH ₃ CH ₂ COCH ₂ CH ₃ ^{i,k}	2902–2173	729	2.09
(CH ₃) ₂ CHCOCH(CH ₃) ₂ ^{j,l}	2930–2153	777	2.22
CH ₃ NO ₂ ^m	2965–2160	805	2.30
HCN ⁿ	3311–2630	681	1.96
CH ₃ SH ^o	2605–1893	712	2.04

^a Vapor unless otherwise stated. ^b Reference 32 and 33. ^c Reference 34. ^d Reference 35. ^e Reference 36. ^f Thin film. ^g Based on $\nu_H/\nu_D = 1.34$. ^h Reference 37 and 38. ⁱ Reference 39. ^j CCl₄ and CS₂, dilute solutions. ^k Reference 40. ^l Reference 41 and 42. ^m Reference 43. ⁿ Reference 44. ^o Reference 45.

perimental open data points with the corresponding solid calculated points is shown in Figure 3. Also shown in Figure 3 is a plot of calculated vs. experimental data points. The low slope (0.632) and poor correlation coefficient (0.62) suggest that factors other than the ΔpK_a value may be important in determining k_H/k_D .

As shown in Figure 1, the point for the k_H/k_D value of HOCH₂CH₂S⁻ is exceptionally high whereas that for acetate is low compared to the other oxyanions. This type of variation which is dependent upon the class of carbon acid or the class of proton-abstracting base is probably responsible for much of the scatter found normally in plots of k_H/k_D vs. ΔpK_a .⁴ Several authors have suggested that the magnitude of the zero-point energy change upon deuteration of both the donor and acceptor atoms (as determined by their force constants) should influence the observed k_H/k_D value.^{4,25} However, this has not been incorporated into a generally useful equation for the prediction of primary deuterium isotope effects for proton transfer involving carbon.

Shown in Figure 4 is the free energy profile for the generalized proton (deuteron)-abstraction reaction $LA + B \rightarrow (A \cdots L \cdots B)^{\ddagger} \rightarrow A + LB$. The magnitude of the zero-point energies in the figure is exaggerated for clarity, and the potential energy well for the vibration of the isotopically substituted atom is different in reactants and products, so that the derived equation will be general. (The corresponding model used to generate eq 2 inherently presumes no difference in the zero-point energy change upon deuteration for reactants and products.) For convenience, the effective free energy for the reaction of the nondeuterated substrate was chosen to be $\Delta G_H^{\circ} = 0$, so that by definition the intrinsic barrier,^{17,18} $\lambda_H/4$, is the activation energy at this point (that is, $\lambda_H/4 = \Delta G_H^{\ddagger}$ at $\Delta G_H^{\circ} = 0$). The free energy of activation of the corresponding deuterated reaction may be defined as

$$\Delta G_D^{\ddagger} = \Delta G_H^{\ddagger} + \Delta\epsilon_R - \Delta\epsilon^{\ddagger}$$

where $\Delta\epsilon^{\ddagger}$ is the zero-point energy change upon deuteration of the transition state.

The bond energy–bond order theory is predicated upon the assumption that the activation energy is a function of the bond energies of both reactants and products.²⁶ It is therefore reasonable to assume that the value of $\Delta\epsilon^{\ddagger}$ is a composite of the ground-state zero-point energy changes upon deuteration of both the reactants and products and can be defined for this special case in Figure 4 as

$$\Delta\epsilon^{\ddagger} = (C/2)(\Delta\epsilon_R + \Delta\epsilon_P)$$

where $\Delta\epsilon^{\ddagger}$ is the zero-point energy change upon deuteration of the transition state when $\Delta G_H^{\circ} = 0$ and C is an empirical constant. Thus defined, C is the ratio of the energy change upon deuteration of the transition state to the average energy change upon deuteration of the reactant and product. If $C = 1.0$, then no isotope

(25) Motell, E. L.; Boone, A. W.; Fink, W. *Tetrahedron* **1978**, *34*, 1619.
(26) Johnston, H. S. "Gas Phase Reaction Rate Theory"; Ronald Press: New York, New York, 1966.

Table III. Primary Isotope Effects for Proton Abstraction from Carbon Acids (Calculated with $\lambda_H/4 = 10$ kcal/mol, $C = 0.4$)

acid	base	ΔpK_a	k_H/k_D exptl	$\Delta \epsilon_R$	$\Delta \epsilon_P$	calcd k_H/k_D	
						eq 2	eq 3
1. $(CH_3)_2C=^+OH$	H_2O^e	2.0	7.0	2.14	2.75	8.36	6.59
2. $O_2NPhOCH_2CH_2COCH_3$	OH^{-b}	0.75	6.0	2.08	2.75	8.55	6.28
3. $O_2NPhOCH_2CH_2COCH_3$	$C_6H_5O^{-b}$	6.64	6.0	2.08	2.73	6.48	4.88
4. $O_2NPhOCH_2CH_2COCH_3$	$CF_3CH_2O^{-b}$	4.13	5.6	2.08	2.75	7.70	5.56
5. $O_2NPhOCH_2CH_2COCH_3$	$CH_3CONHC_6H_4O^{-b}$	7.01	5.8	2.08	2.73	6.28	4.77
6. $O_2NPhOCH_2CH_2COCH_3$	$3,4-Cl_2C_6H_3O^{-b}$	7.99	4.7	2.08	2.73	5.78	4.49
7. $O_2NPhOCH_2CH_2COCH_3$	$3,4,5-Cl_3C_6H_2O^{-b}$	8.82	5.1	2.08	2.73	5.23	4.19
8. $O_2NPhOCH_2CH_2COCH_3$	$CH_3CO_2^{-b}$	11.74	2.7	2.08	2.69	3.58	3.34
9. $O_2NPhOCH_2CH_2COCH_3$	$(CH_3)_3N^b$	6.76	5.2	2.08	2.42	6.42	5.78
10. $O_2NPhOCH_2CH_2COCH_3$	$HOCH_2CH_2S^{-b}$	6.89	8.5	2.08	2.04	6.35	7.16
11. $O_2NPhOCH_2CH_2COCH_3$	NC^{-b}	7.29	~6	2.08	1.96	6.12	7.39
12. $(CH_3CO)_2CH_2$	H_2O^c	10.6	4.5	2.08	2.75	4.20	3.55
13. $CH_2(CO_2CH_2CH_3)_2$	H_2O^d	15.04	2.0	2.08	2.75	2.04	2.22
14. $CH_3COCH_2SO_3^-$	H_2O^e	15.7	2.5	2.08	2.75	1.79	2.05
15. $CH_3COCH_2SO_3^-$	$ClCH_2CO_2^{-e}$	11.5	2.6	2.08	2.69	3.71	3.42
16. $CH_3COCH_2SO_3^-$	$CH_3CO_2^{-e}$	9.6	3.8	2.08	2.69	4.78	4.04
17. $CH_3COCH_2SO_3^-$	$(CH_3)_3CO_2^{-e}$	9.4	4.4	2.08	2.69	4.90	4.10
18. $CH_3COCH_2SO_3^-$	2,6-lutidine ^e	7.4	7.3	2.08	2.29	6.06	6.03
19. $CH_3COCH_2SO_3^-$	HO^{-e}	-2.0	7.4	2.08	2.75	8.36	6.55
20. $CH_3COCH_2CO_2CH_2CH_3$	H_2O^d	12.2	3.5	2.08	2.75	3.33	3.05
21. $CH_3COCHCH_3CO_2CH_2CH_3$	$(CH_3)_3CO_2^{-d}$	8.0	6.5	2.08	2.69	5.71	4.56
22. $CH_3COCHCH_3CO_2CH_2CH_3$	$CH_3CO_2^{-d}$	8.3	5.9	2.08	2.69	5.54	4.47
23. $CH_3COCHCH_3CO_2CH_2CH_3$	$ClCH_2CH_2CO_2^{-d}$	8.9	5.7	2.08	2.69	5.19	4.27
24. $CH_3COCHCH_3CO_2CH_2CH_3$	$ClCH_2CO_2^{-d}$	10.1	5.2	2.08	2.69	4.49	3.87
25. $CH_3COCHCH_3CO_2CH_2CH_3$	$Cl_2CHCO_2^{-d}$	11.7	3.9	2.08	2.69	3.60	3.35
26. $CH_3COCHCH_3CO_2CH_2CH_3$	H_2O^d	14.0	3.8	2.08	2.75	2.47	2.51
27. $CH_3COCHCH_3CO_2CH_2CH_3$	F^{-d}	9.4	3.0	2.08	3.87	4.89	1.89
28. $CH(CO_2CH_3)_3$	H_2O^e	9.4	3.8	2.22	2.75	4.89	4.91
29. $CH(CO_2CH_3)_3$	$ClCH_2CO_2^{-e}$	5.2	5.0	2.22	2.69	7.23	6.68
30. $CH(CO_2CH_3)_3$	$ClCH_2CH_2CO_2^{-e}$	4.0	5.7	2.22	2.69	7.75	7.05
31. $CH(CO_2CH_3)_3$	$CH_3CO_2^{-e}$	3.3	5.5	2.22	2.60	8.01	7.54
32. $CH(CO_2CH_3)_3$	$(CH_3)_3CO_2^{-e}$	3.1	6.6	2.22	2.69	8.07	7.30
33. 2-acetylcyclohexanone	H_2O^e	11.8	4.6	2.22	2.75	3.54	3.97
34. 2-acetylcyclohexanone	$CH_3CO_2^{-e}$	5.7	7.2	2.22	2.69	6.98	6.51
35. 2-acetylcyclohexanone	2,6-lutidine ^e	3.5	10.3	2.22	2.29	7.94	8.63
36. $(CH_3CO)_2CHBr$	H_2O^d	8.3	3.9	2.22	2.75	5.54	5.35
37. $CH_3COCHBrCO_2CH_2CH_3$	H_2O^e	8.3	4.3	2.22	2.75	5.54	5.35
38. 2-carboethoxycyclohexanone	H_2O^e	11.64	4.6	2.22	2.75	3.63	4.04
39. 2-carboethoxycyclopentanone	H_2O^f	12.24	3.4	2.22	2.75	3.31	3.81
40. $CHBr(CO_2CH_2CH_3)_2$	H_2O^c	12.30	2.7	2.22	2.75	3.28	3.78
41. $O_2NCH_2CO_2CH_2CH_3$	H_2O^e	7.7	3.6	2.08	2.75	5.89	4.49
42. $O_2NCH_2CO_2CH_2CH_3$	$ClCH_2CO_2^{-e}$	3.5	6.6	2.08	2.69	7.94	5.87
43. $O_2NCH_2CO_2CH_2CH_3$	$CH_3CO_2^{-e}$	1.6	7.7	2.08	2.69	8.44	6.28
44. $O_2NCH_2CO_2CH_2CH_3$	2-methylpyridine ^e	0.1	9.6	2.08	2.29	8.58	7.48
45. $O_2NCH_2CO_2CH_2CH_3$	4-methylpyridine ^e	0.1	9.1	2.08	2.29	8.58	7.48
46. $O_2NCH_2CO_2CH_2CH_3$	2,6-lutidine ^e	-0.6	9.9	2.08	2.29	8.56	7.50
47. $O_2NCH_2CO_2CH_2CH_3$	2- $ClC_6H_4O^{-e}$	-2.3	8.1	2.08	2.73	8.29	6.59
48. $O_2NCH_2CO_2CH_2CH_3$	$C_6H_5O^{-e}$	-3.9	6.7	2.08	2.73	7.79	6.58
49. $O_2NCH_2CO_2CH_2CH_3$	HO^{-e}	-10.0	4.6	2.08	2.75	4.55	5.54
50. CH_3NO_2	HO^{-d}	-5.3	10.3	2.30	2.75	7.18	8.34
51. CH_3NO_2	$CH_3CO_2^{-d}$	6.2	6.5	2.30	2.69	6.72	7.15
52. CH_3NO_2	$ClCH_2CO_2^{-d}$	8.1	4.3	2.30	2.69	5.65	6.37
53. CH_3NO_2	H_2O^d	12.0	3.8	2.30	2.75	3.44	4.40
54. $CH_3CH_2NO_2$	$CF_3CH_2NH_2^f$	2.97	7.2	2.30	2.42	8.11	9.25
55. $CH_3CH_2NO_2$	1,2-diaminopropane ^g	1.47	8.3	2.30	2.42	8.46	9.51
56. $CH_3CH_2NO_2$	glycine ethyl ether ^g	0.85	7.5	2.30	2.42	8.54	9.58
57. $CH_3CH_2NO_2$	Tris ^g	0.45	8.5	2.30	2.42	8.57	9.61
58. $CH_3CH_2NO_2$	glycylglycine ^g	0.2	9.6	2.30	2.42	8.57	9.62
59. $CH_3CH_2NO_2$	NH_3^g	-0.73	10.0	2.30	2.42	8.55	9.63
60. $CH_3CH_2NO_2$	glycine ^g	-1.03	7.8	2.30	2.42	8.52	9.63
61. $CH_3CH_2NO_2$	piperidine ^g	-2.50	8.1	2.30	2.42	8.24	9.52
62. $CH_3CH_2NO_2$	HO^{-h}	-7.15	9.3	2.30	2.75	6.20	7.89
63. $CH_3CH_2NO_2$	$CH_3CO_2^{-h}$	3.84	5.9	2.30	2.69	7.81	7.98
64. $C_6H_5CH_2NO_2$	HO^{-i}	-8.94	7.4	2.30	2.75	5.16	7.30
65. $C_6H_5CH_2NO_2$	piperidine ⁱ	-4.32	8.5	2.30	2.42	7.62	9.20
66. $C_6H_5CH_2NO_2$	ethylamine ^e	-4.0	10.5	2.30	2.42	7.75	9.27
67. $C_6H_5CH_2NO_2$	morpholine ^e	-1.53	9.3	2.30	2.42	8.45	9.60
68. $C_6H_5CH_2NO_2$	Tris ⁱ	-1.35	10.6	2.30	2.42	8.48	10.01
69. $C_6H_5CH_2NO_2$	imidazole ⁱ	-0.45	11.5	2.30	2.29	8.57	10.06
70. $C_6H_5CH_2NO_2$	acetate ^e	2.55	8.3	2.30	2.69	8.23	8.33
71. $C_6H_5CH_2NO_2$	HCO_2^{-i}	3.35	7.3	2.30	2.69	7.99	8.12
72. $C_6H_5CH_2NO_2$	$ClCH_2CO_2^{-i}$	4.25	7.4	2.30	2.69	7.65	7.85
73. $C_6H_5CH_2NO_2$	H_2O^j	8.54	5.5	2.30	2.75	5.40	5.95
74. $C_6H_5CH_2NO_2$	F^{-i}	3.62	4.8	2.30	3.87	7.89	4.70
75. $C_6H_5CH_2NO_2$	2,6-lutidine ^j	-0.9	12.3	2.30	2.29	8.53	10.04

Table III (Continued)

acid	base	ΔpK_a	k_H/k_D exptl	$\Delta\epsilon_R$	$\Delta\epsilon_P$	calcd k_H/k_D	
						eq 2	eq 3
76. $(CH_3)_2CHNO_2$	HO^{-i}	-8.3	7.4	2.30	2.75	5.54	7.52
77. $(CH_3)_2CHNO_2$	pyridine ^f	2.5	10.3	2.30	2.29	8.24	9.88
78. $(CH_3)_2CHNO_2$	$CH_3CO_2^{-i}$	3.3	7.6	2.30	2.69	8.01	8.13
79. nitrocyclohexane	HO^{-i}	-7.4	7.6	2.30	2.75	6.06	7.82

^a Reference 46. ^b This study. ^c Reference 5. ^d Reference 6. ^e Reference 47. ^f Reference 8. ^g Reference 9. ^h Reference 48. ⁱ Reference 11.

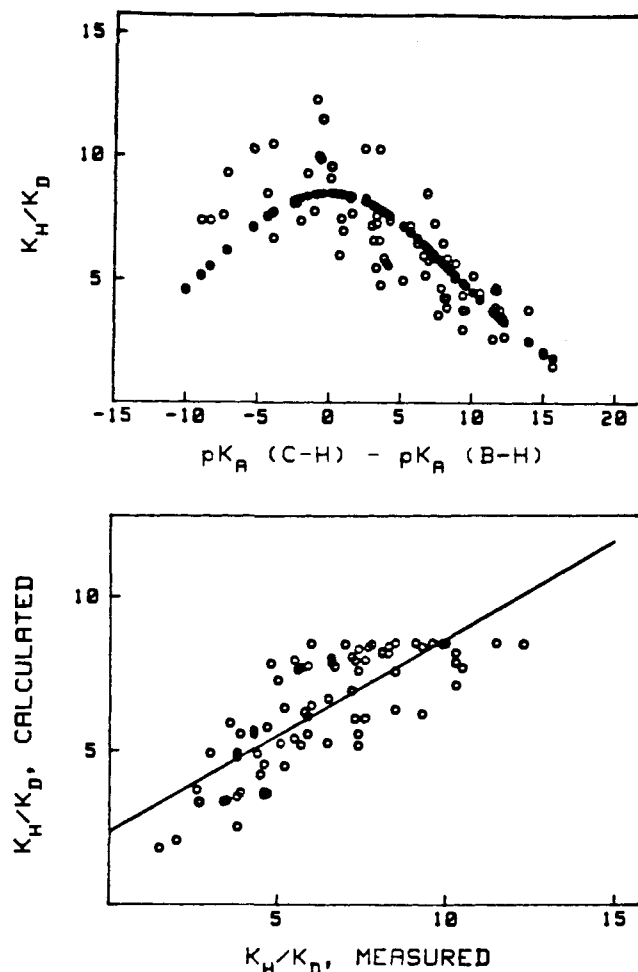


Figure 3. The upper plot shows the experimental values of k_H/k_D (O) vs. ΔpK_a listed in Table III, along with those calculated (●) with eq 2 with $\lambda_H/4 = 5.85$ and $(k_H/k_D)_{max} = 8.58$. The lower panel shows a plot of calculated vs. measured values of k_H/k_D with a slope of 0.632 and $r^2 = 0.622$.

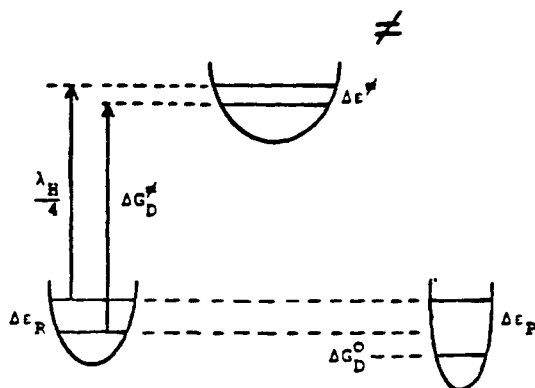


Figure 4. A free energy profile for the generalized proton (deuteron) abstraction reaction. The free energy for the reaction of the nondeuterated substrate was chosen to be $\Delta G_H^\circ = 0$.

effect will be found at $\Delta G^\circ = 0$, and if $C = 0$ a maximal isotope effect will be found. This adjustable parameter is analogous to

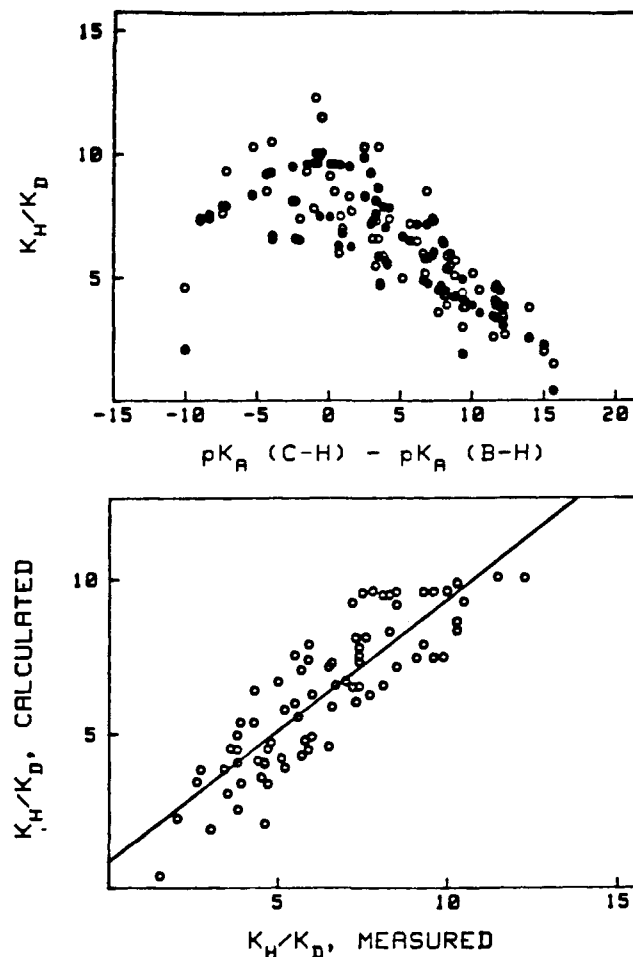


Figure 5. The upper panel shows a plot of the experimental k_H/k_D values (O) from Table III along with values calculated (●) with use of eq 3 with $C = 0.4085$ and $\lambda_H/4 = 8.41$. The lower panel shows a plot of calculated vs. experimental values of k_H/k_D with a least-squares slope of 0.840 and $r^2 = 0.755$.

$(k_H/k_D)_{max}$ in eq 2. Although it is obviously an approximation to presume that the zero-point energy changes in the transition state are a constant fraction of the average of those in the group state, this simplifying presumption provides a practical means of incorporating this parameter into a calculated value of k_H/k_D .

It is possible to define the intrinsic barrier for the reaction of the deuterated substrate in terms of the intrinsic barrier for the reaction of the nondeuterated substrate and zero-point energy changes upon deuteration of the reactants and products:

$$\lambda_H/4 + \Delta\epsilon_R - \frac{C}{2}(\Delta\epsilon_R + \Delta\epsilon_P) = \frac{\lambda_D}{4} \left(1 + \frac{\Delta\epsilon_R - \Delta\epsilon_P}{\lambda_D} \right)^2$$

Solving for the intrinsic barrier $\lambda_D/4$ gives:

$$\lambda_D/4 = \{4p + (16p^2 - 4b^2)^{1/2}\}/8$$

where $p = \lambda_H/4 + 1/2(1 - C)(\Delta\epsilon_R + \Delta\epsilon_P)$ and $b = (\Delta\epsilon_R - \Delta\epsilon_P)$. In terms of the Marcus equation

$$\Delta G_H^\ddagger = w_H^\ddagger + (\lambda_H/4)(1 + \Delta G_H^\circ/\lambda_H)^2$$

and for the deuteron transfer reaction

$$\Delta G_D^\ddagger = w_D + \frac{\lambda_D}{4} \left(1 + \frac{\Delta G_H^\circ + \Delta \epsilon_R - \Delta \epsilon_P}{\lambda_D} \right)^2$$

The kinetic isotope effects arise from a difference in the activation energies for these reactions, where, if it is presumed that $W_r^D = W_r^H$,

$$k_H/k_D = \exp[(\Delta G_D^\ddagger - \Delta G_H^\ddagger)/RT] = \exp \left[\frac{\lambda_D}{4} \left(1 + \frac{\Delta G_H^\circ + \Delta \epsilon_R - \Delta \epsilon_P}{\lambda_D} \right)^2 - \frac{\lambda_H}{4} \left(1 + \frac{\Delta G_H^\circ}{\lambda_H} \right)^2 \right] / RT \quad (3)$$

From this equation it is possible to predict an isotope effect if the intrinsic barrier for the proton transfer reaction and the zero-point energy changes upon deuteration of the reactant and products are known. Table II contains the stretching frequencies of model compounds which may be used to determine the zero-point energy change upon deuteration of reactants and products. Although it is true that these stretching frequencies contribute substantially to the total zero-point energies, it is also certainly true that contributions from other vibrational modes make a significant contribution to the zero-point energies. The application of eq 3 assumes that differences in stretching frequency upon deuteration dominate the isotope effect measured.

The data in Table III were fit to eq 3 by using an SAS nonlinear least-squares program with two adjustable parameters, $\lambda_H/4$ and C . The best fit was obtained with $\lambda_H/4 = 8.41$ kcal/mol and $C = 0.408$. Shown in Figure 5 are the experimental and calculated values of k_H/k_D vs. pK_a . The calculated points show scatter vs. ΔpK_a since their magnitudes depend upon the infrared frequency shift data as well as ΔpK_a .

The higher slope (0.84) and better correlation coefficient (0.76) of this plot compared to those shown in Figure 3 suggest that although the magnitude of the isotope effect is dominated by the ΔpK_a value, the zero-point energy changes upon deuteration of reactants and products also has an influence. In eq 2, it was inherently assumed that $\Delta G_H^\circ = \Delta G_D^\circ$. This is equivalent to assuming that there will be no isotope effect on the free energy of the reaction (that is, $\Delta \epsilon_R - \Delta \epsilon_P = 0$). This will certainly not be generally true, and the isotope effect on the equilibrium, as shown by the improved correlation coefficient and slope, does make a significant contribution to the magnitude of the kinetic isotope effects. It is also true, however, that substantial scatter still exists in Figure 5, so that other factors not accounted for in eq 3 may be contributing to the observed value of k_H/k_D . These factors include tunneling and the possible variation in λ for various carbon acids, as well as contributions of other vibrational modes.

From the data in Table II, it is apparent that the differences in $(\Delta \epsilon_R - \Delta \epsilon_P)$ are comparable when using oxyanion and amine bases and therefore, the choice of $\log(k_H/k_D)_{\max} = 8.5$ in eq 2 fairly adequately predicts the values of k_H/k_D for these classes of bases, as shown in Figure 3. However, this correlation between the calculated and experimental values tends to obscure the importance of the type of base used to abstract the proton. For example, fluoride ion has an unusually large zero-point energy change upon deuteration ($\Delta \epsilon = 3.87$ kcal/mol for hydrogen fluoride compared to $\Delta \epsilon = 2.73$ kcal/mol for phenol). The data in Table III show that eq 3 is better than eq 2 for this particular base, predicting 1.89 instead of 4.89 in one case (measured 3.0) and 4.70 instead of 7.89 in another (measured 4.7). An improvement was also found in the predicted value (7.16 rather than 6.35) for thiol anion catalyzed proton abstraction (measured 8.5). Thiols have an unusually small zero-point energy change upon deuteration ($\Delta \epsilon = 2.04$ kcal/mol for methanethiol compared to $\Delta \epsilon = 2.73$ kcal/mol for phenol). If the data in Table III and Figures 3 and 5 had contained a larger variety of bases such as a more representative collection of fluoride ion and thiol anion data, the correlation between the experimental values of k_H/k_D and those calculated by using eq 2 would have been worse, and the improvement by using eq 3 would have been even more substantial. Shown in Figure 6 are curves computed for k_H/k_D

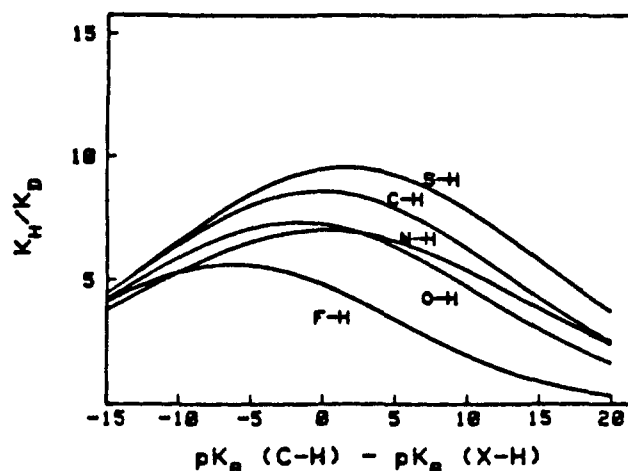


Figure 6. Values of k_H/k_D vs. ΔpK_a calculated with eq 3 for different base types with the following typical values for constants: $\lambda_H/4 = 8.41$, $C = 0.4085$, $\epsilon_r(\text{C-H}) = 2.15$ kcal/mol, $\Delta \epsilon_P(\text{C-H}) = 2.15$, $\Delta \epsilon_P(\text{N-H}) = 2.35$, $\Delta \epsilon_P(\text{O-H}) = 2.70$, $\Delta \epsilon_P(\text{F-H}) = 3.87$, and $\Delta \epsilon_P\text{-S-H} = (2.04)$ kcal/mol.

for proton abstraction by various classes of bases. These curves demonstrate that the change in the identity of the atom doing the proton abstraction alters the ΔpK_a value at which the maximum is reached, as well as altering the maximal k_H/k_D value. The low values found experimentally for fluoride are due in large part to the fact that the maximum value of k_H/k_D occurs some 6 pK_a units away from zero.

There is a correspondence between the conclusions reached in this study for proton transfer and those reached for acyl transfer reactions.²⁷⁻³⁰ It has been previously shown that oxyanions exhibit curved β_{nuc} plots for attack on acyl carbon whereas thiol anions do not.²⁷⁻²⁹ We have ascribed this oxyanion curvature to the same solvation source for both nucleophilic and proton transfer reactions. Recently we have shown that in the region where β_{nuc} varies substantially for oxyanion attack on formyl or deuterioformyl esters, there is no measurable change in the secondary deuterium isotope effect.³⁰ Therefore, it appears that for proton transfer from both carbon and acyl transfer reactions, transition-state structure changes and the corresponding isotope effect changes are small over the range of reactivity generated by changing the pK_a of the base or nucleophile. The curvature found in β or β_{nuc} plots for oxyanions is absent for thiol anions and is caused by an effect due to solvation. This also implies that the use of β values to determine the degree of bond formation is not appropriate for oxyanions acting as nucleophiles or as proton abstractors from carbon in aqueous solution, unless the β values are measured by varying the electrophile or carbon acid with a homologous series of bases.

- (27) Hupe, D. J.; Jencks, W. P. *J. Am. Chem. Soc.* **1977**, *99*, 451.
- (28) Hupe, D. J.; Wu, D.; Sheppard, P. *J. Am. Chem. Soc.* **1977**, *99*, 7659.
- (29) Pohl, E. R.; Wu, D.; Hupe, D. J. *J. Am. Chem. Soc.* **1980**, *102*, 2759.
- (30) Pohl, E. R.; Hupe, D. J. *J. Am. Chem. Soc.* **1980**, *102*, 2763.
- (31) Hall, H. K. *J. Am. Chem. Soc.* **1957**, *79*, 5441.
- (32) Adams, R. M.; Katz, J. J. *J. Opt. Soc. Am.* **1956**, *46*, 895.
- (33) Spanbauer, R. N.; Rao, K. N.; Jones, L. H. *J. Mol. Spectrosc.* **1965**, *16*, 100.
- (34) Haurie, M.; Novak, A. *J. Chem. Phys.* **1965**, *62*, 137.
- (35) Faulk, M.; Whalley, E. *J. Chem. Phys.* **1961**, *34*, 1554.
- (36) Evans, J. C. *Spectrochim. Acta* **1960**, *16*, 1382.
- (37) Waddington, T. C. *J. Chem. Soc.* **1958**, 4340.
- (38) Nuttall, R. H.; Sharp, D. W.; Waddington, T. C. *J. Chem. Soc.* **1960**, 4965.
- (39) Dellepiane, G.; Overend, J. *J. Spectrochim. Acta* **1966**, *22*, 593.
- (40) Nolin, B.; Jones, R. N. *J. Am. Chem. Soc.* **1953**, *75*, 5627.
- (41) Karabatsos, G. J. *J. Org. Chem.* **1960**, *25*, 315.
- (42) "Documentation of Molecular Spectroscopy"; Butterworths Scientific Publications: London, 1967.
- (43) Wilson, T. P. *J. Chem. Phys.* **1943**, *11*, 361.
- (44) Mann, R. H.; Horrocks, W. D., Jr. *J. Chem. Phys.* **1966**, *45*, 1278.
- (45) May, I. W.; Pace, E. L. *Spectrochim. Acta, Part A* **1968**, *24A*, 1605.
- (46) Toulke, J.; Dubois, J. E. *J. Am. Chem. Soc.* **1974**, *96*, 3524.
- (47) Barnes, D. J.; Bell, R. P. *Proc. R. Soc. London, Ser. A* **1970**, *318*, 421.
- (48) Davis, M. H. *J. Chem. Soc., Perkin Trans. 2* **1974**, 1018.